

**LOW NOISE HgCdTe 128 X 128 SWIR FPA  
FOR HUBBLE SPACE TELESCOPE**

Michael Blessinger and Kadri Vural  
Rockwell International Science Center  
Thousand Oaks, CA 91360

William Kleinhans  
Valley Oak Semiconductor  
Westlake Village, CA 91362

Marcia Rieke, Rodger Thompson and Robert Rasche  
University of Arizona  
Tucson, AZ 85721

**Abstract**

Large area focal plane arrays of unprecedented performance have been developed for use in NICMOS, a proposed Hubble Space Telescope refurbishment instrument. These FPAs are 128x128-element, HgCdTe hybrid arrays with a cutoff wavelength of 2.5  $\mu\text{m}$ . The multiplexer consists of a CMOS FET switch array with a typical mean readout noise of less than 30 electrons. The detectors typically have a mean dark current of less than 10 electrons/s at 77K, with currents below 2 electrons/s measured at 60K (both at 0.5 V reverse bias). The mean quantum efficiency is 40-60% at 77K for 1.0-2.4  $\mu\text{m}$ . Functional pixel yield is typically greater than 99%, and the power consumption is approximately 0.2 mW (during readout only).

**Focal plane array design**

The NICMOS focal plane array (FPA) is a hybrid structure consisting of a silicon multiplexer mated through indium columns to a HgCdTe detector array. The detectors are an array of photodiodes formed by ion implantation in a layer of HgCdTe grown by liquid phase epitaxy on a substrate of sapphire. The bandgap of the detector material is chosen such that it responds to infrared radiation in the 0.8 to 2.5  $\mu\text{m}$  wavelength region. The format of the array is 128 x 128 elements on 60  $\mu\text{m}$  centers.

Each detector is connected to a source follower amplifier in the input cell of the multiplexer through an indium column. This amplifier can be connected to the multiplexer output amplifier through a set of row and column select switches (Figure 1). In normal operation, the reset FETs, M2 and M4, are turned on to reset the voltage at the cathode of the detector, and are then turned off, allowing the cathode to float. Photo and dark current is then integrated into that capacitance which is the sum of the detector capacitance and the input capacitance of the multiplexer. Since the detector substrate voltage is fixed, the cathode voltage (and thus the voltage at the gate of the source follower M1) changes, reflecting the integrated current. Since the integration capacitance is small (approximately 0.1 pf), a small amount of integrated charge produces a significant voltage

change at the source follower gate. When M3 and M5 are turned on, the voltage at the unit cell source follower is sampled at the output amplifier, which is another source follower.

Control of the select and reset switches, M2 through M5, is accomplished by the operation of two shift registers driven by user supplied clocks. Additionally, the reset is gated by an enable line, REN, which allows one to optionally reset or not reset a particular pixel while it is selected. This not only allows monitoring of the reset level at the output, but also allows the pixel to be sampled non-destructively. Consequently, sophisticated sampling schemes can be used to improve the signal-to-noise ratio.

Since the multiplexer is CMOS in design, and because the input cell source follower only draws power when it is accessed, the design is inherently low power. Turning off the output amplifier when readout is not occurring reduces power consumption to zero. During readout, only the output amplifier and one input cell amplifier are on at any time, so that the power consumed is a minimal 0.2 mW when 5V power supplies are used.

### Performance results

Completed focal plane arrays were tested extensively with particular attention paid to their noise and dark current characteristics.

**Dark current.** The dark current was characterized at a wide variety of reverse biases at 77K. Figure 2 shows a dark current histogram at 79K and 0.5 V reverse bias which has a mean value of 4.3 electrons/s. Figure 3 shows the mean array dark current versus bias at 79K. Even at large biases of several volts, currents less than 100 electrons/s were achieved. At 60K the dark current is even lower as shown in Fig. 4 where it is 1.6 electrons/s ( $10^{-19}$  amps).

**Noise.** The multiplexer readout noise was characterized in a variety of readout schemes. A simple model of the multiplexer circuit based on 1/f and thermal MOSFET noise indicates that the noise level should be about 4 electrons distributed fairly equally between the input cell amplifier and the output amplifier. Since this represents a level of about 3  $\mu$ V, in practice other sources such as switching transients and crosstalk will in fact dominate.

Three sampling schemes were examined. By sampling the signal, without any multiple sampling, one would expect the noise to be dominated by the reset kTC noise of the integration capacitance, about 60 electrons, which is indeed the case. By sampling both the signal level and the reset pedestal immediately following, one would expect some suppression of low frequency noise, but no removal of the reset noise since the samples are not truly correlated. This results in a noise somewhat worse than the preceding case due to the two samples.

A better sampling scheme is triple correlated sampling where the pixel is sampled immediately before, during, and immediately after reset. By properly correlating samples between frames, a removal of reset kTC noise is accomplished. In this way noise levels below 30 electrons are achieved (Figure 5). From this data a total FPA noise based upon readout noise and dark current can be projected (Figure 6).

**Quantum efficiency.** The mean FPA quantum efficiency was measured at various wavelengths using bandpass filters, and the results are shown in Figure 7.

### Conclusions and future work

The FPAs developed for the NICMOS program have achieved an unprecedented level of performance for a large format array. Readout noises under 30 electrons and dark currents under 10 electrons/s at 77K ( $<2e-/s$  at 60K) were achieved using a design which was simple, easy to operate, and easy to produce. Furthermore, the design can be extrapolated to larger sizes (256x256 for example) with low risk and similar performance.

### Acknowledgements

The authors thank their colleagues at Rockwell for their work in fabricating the FPAs, particularly Jenkon Chen, Victor Johnson, and Matthias Blume. This work was funded by NASA (NAS5-30008) through the University of Arizona NICMOS project.

# NICMOS MULTIPLEXER SCHEMATIC

SC46508

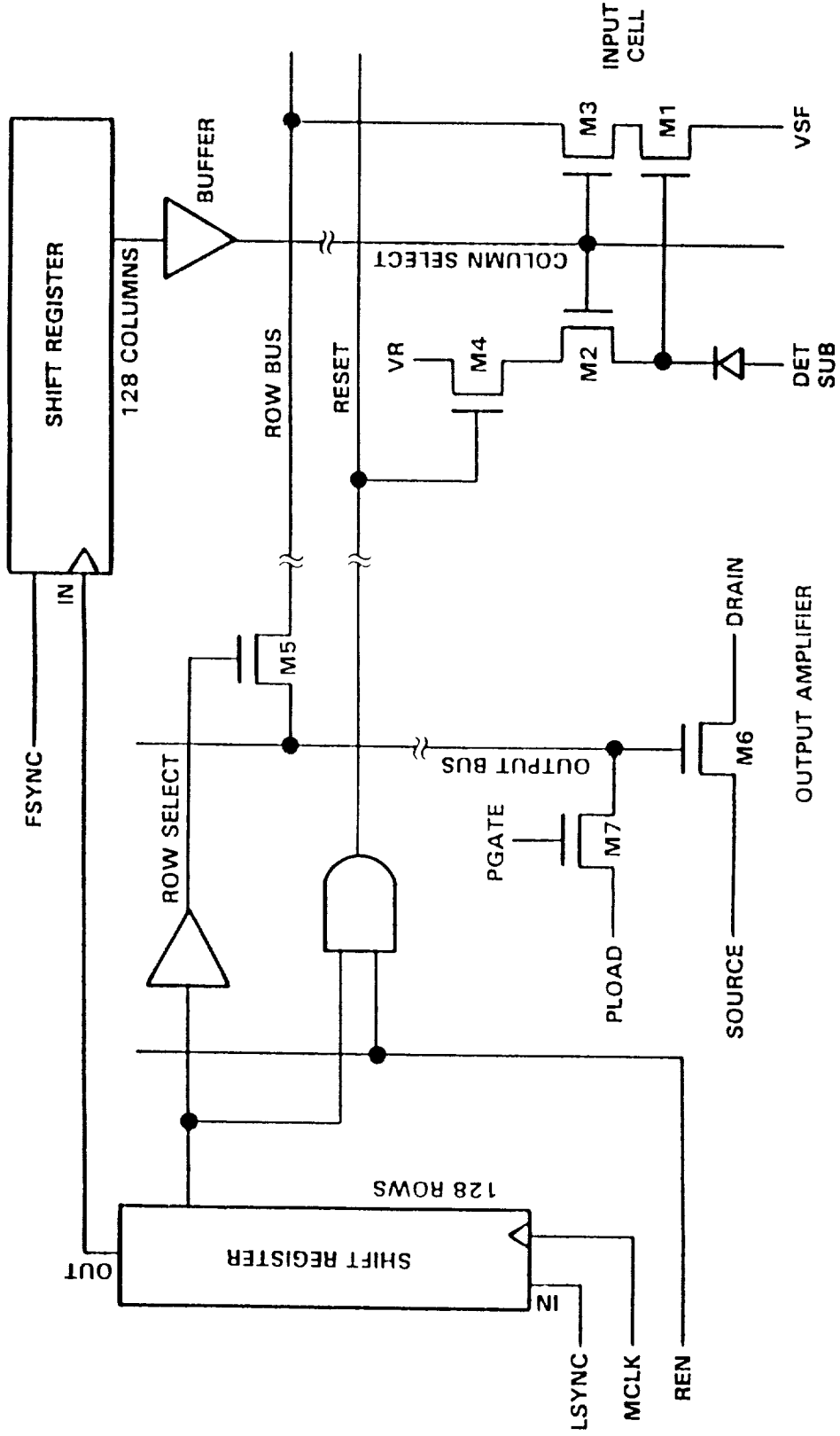


FIGURE 1. NICMOS 128x128 Multiplexer Schematic

# NICMOS 128x128 FPA

SC48505

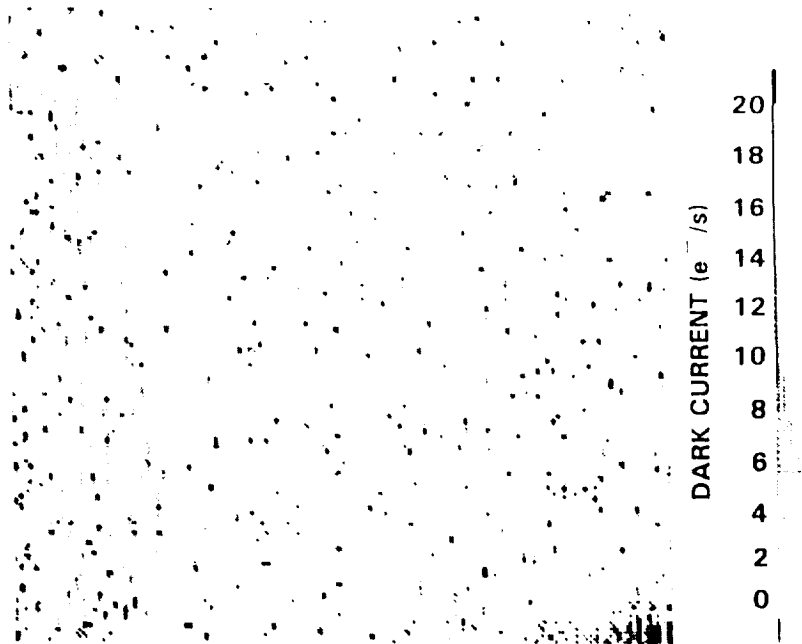
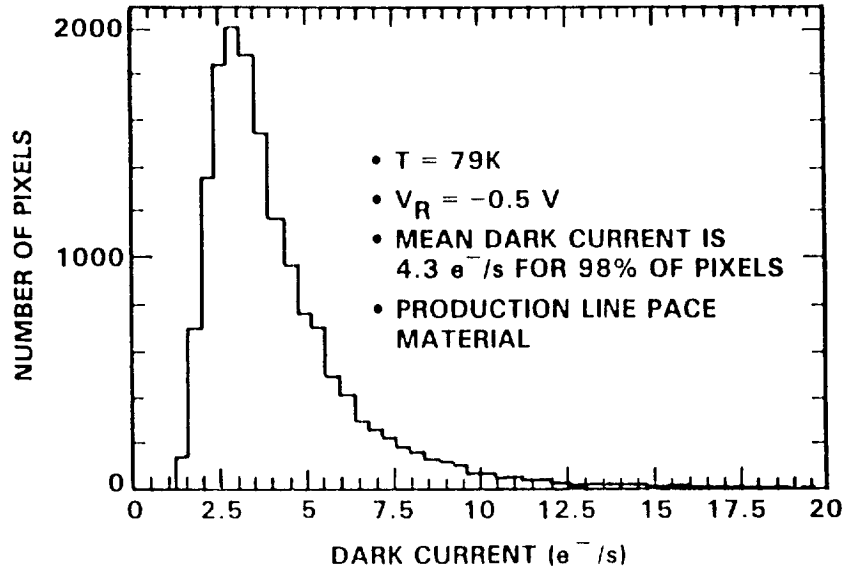


FIGURE 2. Dark current histogram (top) and map (bottom) for NICMOS 128x128 FPA at  $T = 79K$ . There is  $-0.5V$  bias on the detectors. The PACE-1 material has been grown by our production line at Anaheim (EOC).

NICMOS 128x128 FPA  
**MEAN DARK CURRENT AS A FUNCTION OF  
REVERSE BIAS**

SC46502

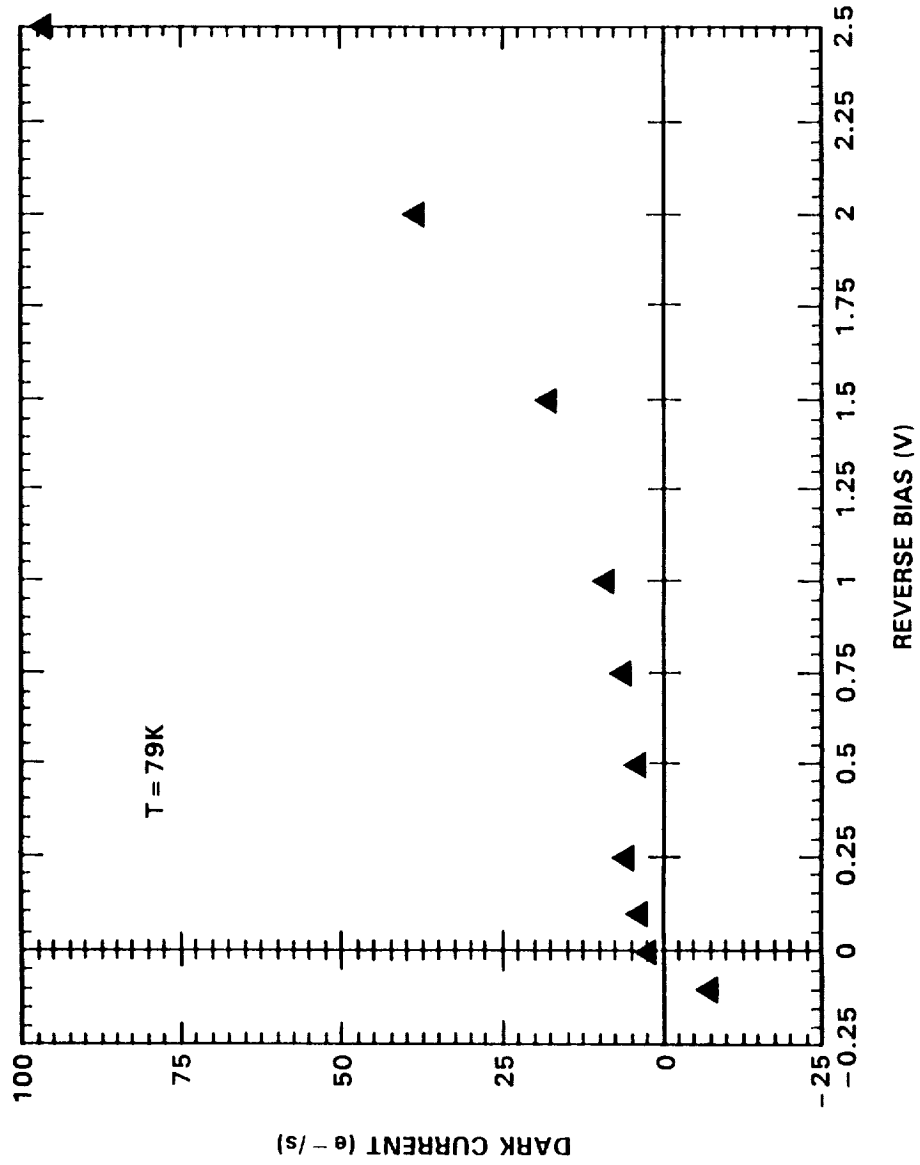
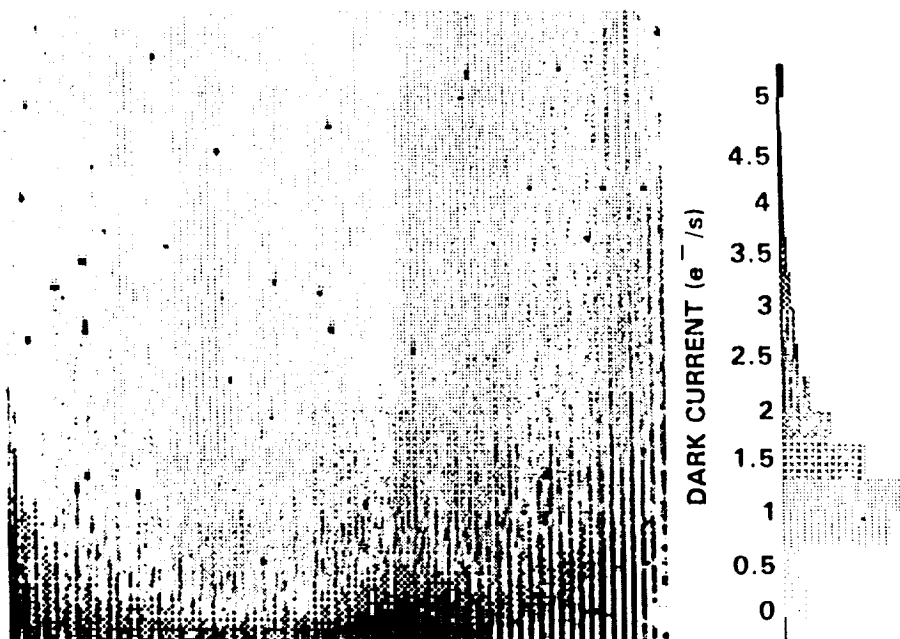
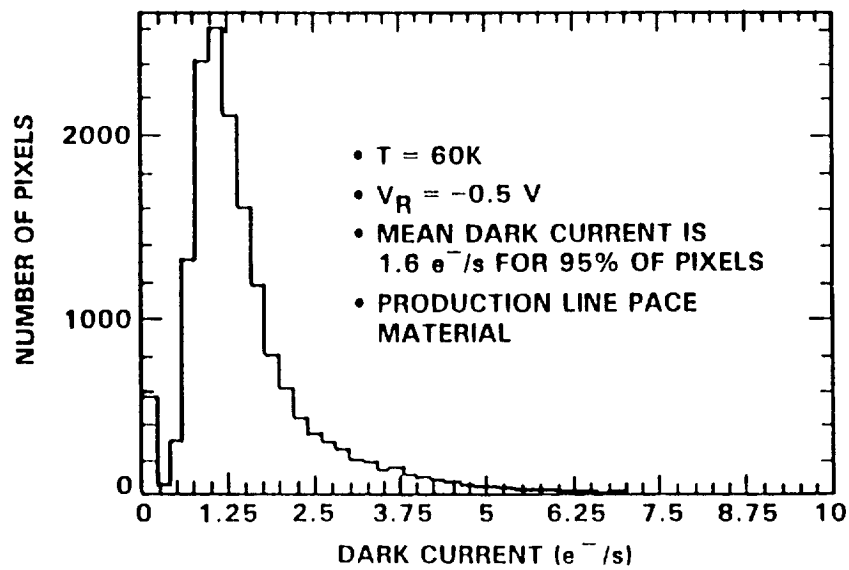


FIGURE 3. NICMOS 128x128 FPA mean dark current as a function of reverse bias at T = 79K.

# NICMOS 128x128 FPA

SC46506



ORIGINAL PAGE IS  
OF POOR QUALITY

FIGURE 4. Dark current histogram (top) and map (bottom) for the same NICMOS 128x128 FPA of Figure 2 at T = 60K. There is some light leakage in the dewar as seen at the bottom portion of the map.

# NICMOS 128x128 FPA

## NOISE vs INTEGRATION TIME

SC46507

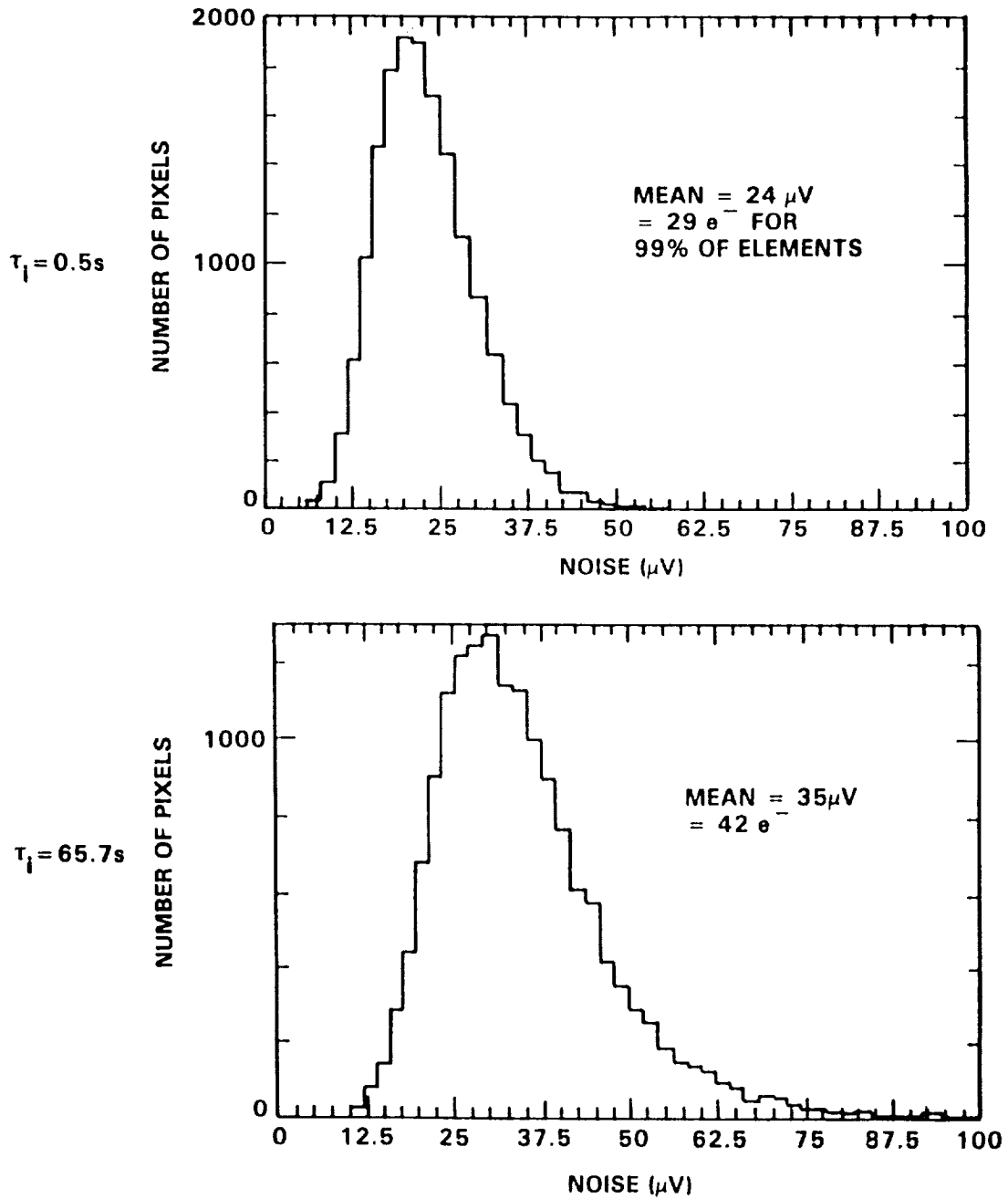


FIGURE 5. Noise histogram for 0.5s and 65.7s integration times.



# PROJECTED FPA NOISE

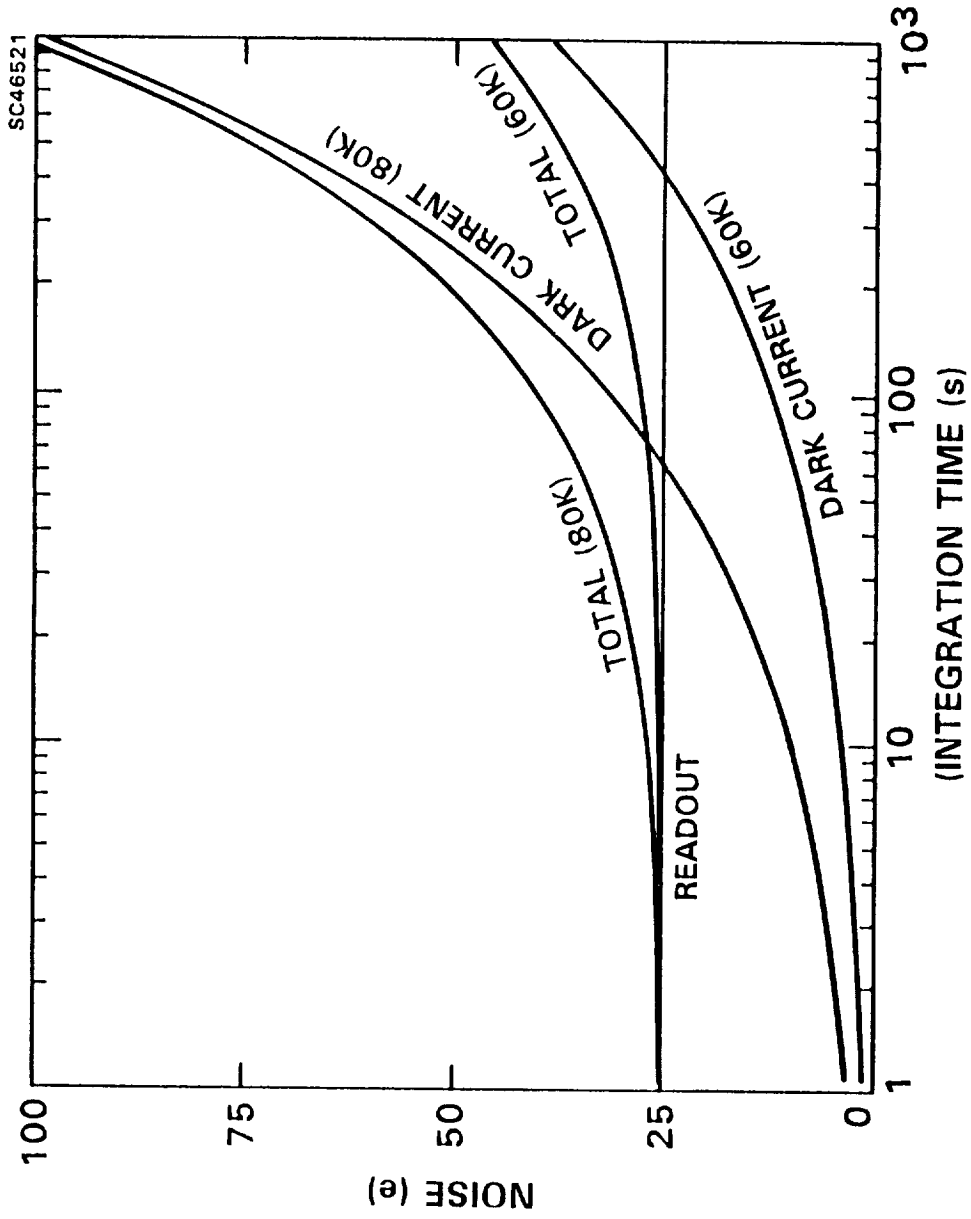


FIGURE 6. Total projected noise (readout plus dark current shot noise) as a function of integration time at 60K and 80K.

# DETECTOR QUANTUM EFFICIENCY

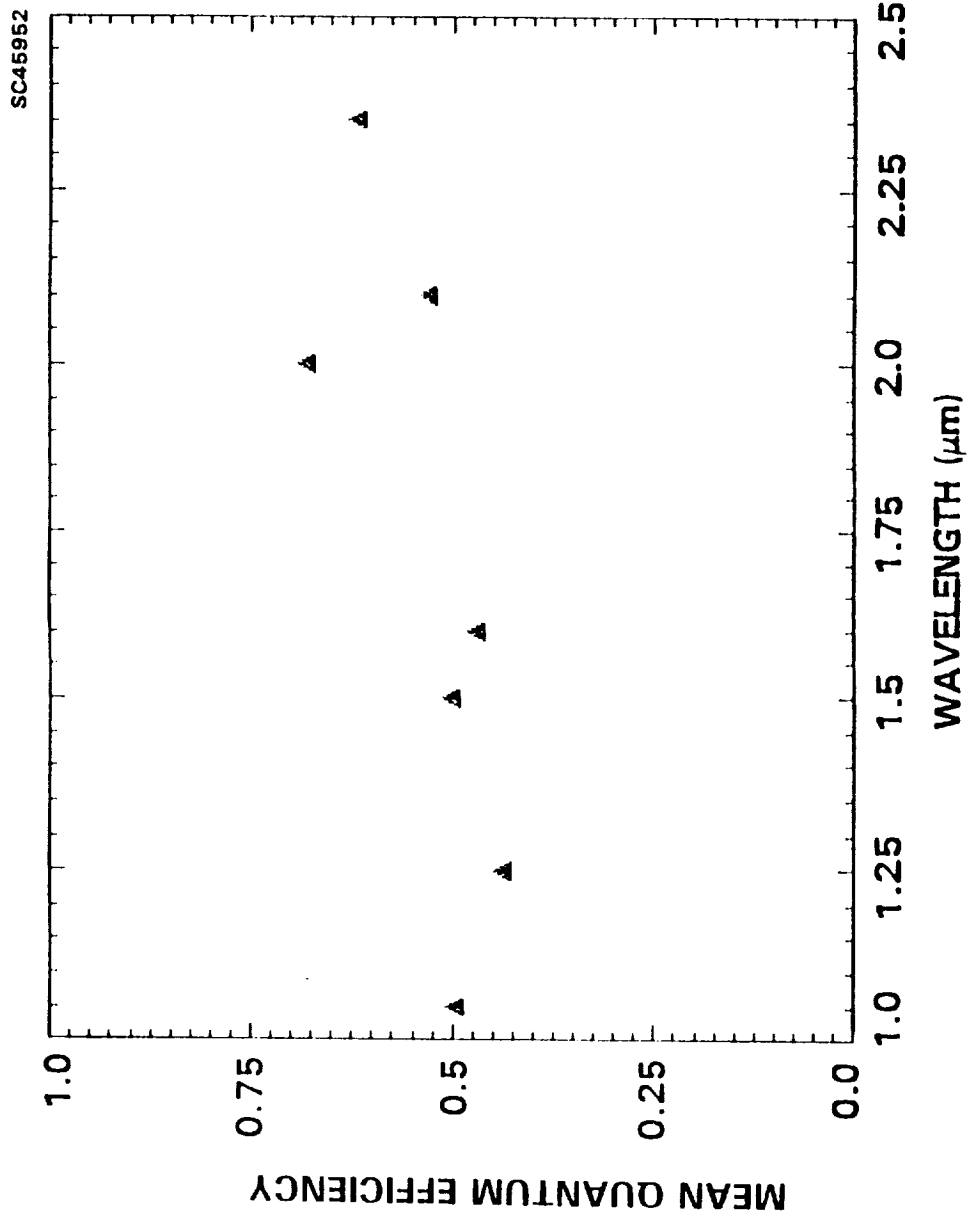


FIGURE 7. Mean quantum efficiency as a function of wavelength for NICMOS 128x128 FPA.